

Dielectric relaxations in ultrathin isotactic PMMA films and PS–PMMA–PS trilayer films

M. Wübbenhorst¹, C.A. Murray², and J.R. Dutcher²

¹ Delft University of Technology, Department of Polymer Materials and Engineering, Julianalaan 136, 2628BL Delft, The Netherlands

² Department of Physics, University of Guelph, Guelph, Ontario, Canada N1G 2W1

Received January, 2003

Published online November 5, 2003 © EDP Sciences / Società Italiana di Fisica / Springer-Verlag 2003

Abstract. The local and cooperative dynamics of supported ultrathin films ($L = 6.4 - 120$ nm) of isotactic poly(methyl methacrylate) (i-PMMA, $\overline{M}_n = 118 \times 10^3$ g/mol) was studied using dielectric relaxation spectroscopy for a wide range of frequencies (0.1 Hz to 10^6 Hz) and temperatures (250–423 K). To assess the influence of the PMMA film surfaces on the glass transition dynamics, two different sample geometries were employed: a single layer PMMA film with the film surfaces in direct contact with aluminum films which act as attractive, hard boundaries; and a stacked polystyrene-PMMA-polystyrene trilayer film which contains diffuse PMMA–PS interfaces. For single layer films of i-PMMA, a decrease of the glass transition temperature T_g by up to 10 K was observed for a film thickness $L < 25$ nm (comparable to R_{EE}), indicated by a decrease of the peak temperature T_α in the loss $\epsilon''(T)$ at low and high frequencies and by a decrease in the temperature corresponding to the maximum in the apparent activation energy $E_a(T)$ of the α -process. In contrast, measurements of i-PMMA sandwiched between PS-layers revealed a slight (up to 5 K) increase in T_g for PMMA film thickness values less than 30 nm. The slowing down of the glass transition dynamics for the thinnest PMMA films is consistent with an increased contribution from the less mobile PMMA–PS interdiffusion regions.

PACS. 64.70.Pf Glass transition – 77.22.Gm Dielectric loss and relaxation

1 Introduction

Recently, the dependence of the glass transition temperature T_g on the thickness of ultrathin polymer films has been studied extensively using a variety of techniques including ellipsometry [1,2,3], Brillouin light scattering (BLS) [4,5,6], X-ray reflectivity [7,8] and dielectric relaxation spectroscopy (DRS) [9,10,11]. The large body of results obtained for both supported and freely-standing polymer films has revealed the influence of the free surface, the underlying substrate, and confinement effects on the measured T_g value. Different mechanisms have been proposed to describe the variety of experimental results, including: (i) segregation of chain ends to the free surface [12,13]; (ii) near-surface cooperative motion [14]; (iii) coupling to capillary modes [15]; (iv) a new type of mobility (“sliding” mode) [16]; (v) reduction of intermolecular coupling and chain orientation near a surface [17,18]; and (vi) percolation of regions of slow dynamics [19]. Although each of the proposed models can be used to explain a subset of the freely-standing and supported polymer film T_g data, none of the proposed models can describe quantitatively all of the data. In addition, it has been suggested that the non-equilibrium nature of

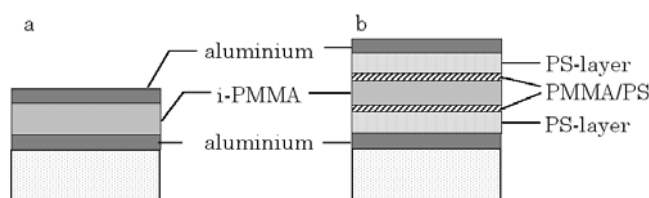


Fig. 1. Schematic sample geometry of a PMMA single layer film and a PS–PMMA–PS trilayer film with aluminium electrodes for DRS experiments.

spincoated films could account for some of the observed behavior [20,21], although it has been shown recently that reductions in T_g with decreasing film thickness cannot be due to reduced entanglement concentrations in spincoated polymer films [22,23].

Dielectric relaxation spectroscopy (DRS) is a particularly suitable technique for the study of dynamics in ultrathin films because of its broad dynamic range and because the capacitance measured in the DRS experiment is inversely proportional to the sample thickness L such that the DRS signal increases as L is decreased. Recently, we have used DRS to study the dynamics in ultrathin

polymer single layer (SL) films ($4 < L < 150$ nm) of stereoregular poly(methyl methacrylate) (PMMA) which were prepared in a sandwich configuration (Al-electrode | PMMA film | Al-electrode) [10]. For all tacticities, we observed systematic changes in the local (β -process) and the cooperative (α -process) dynamics upon reduction of the film thickness. A decrease of the glass transition temperature, T_g , by up to 10 K was observed for a film of i-PMMA of thickness between 25 nm (comparable to the end-to-end distance, R_{EE} , of the polymer coil in bulk) and 6.4 nm. Further reduction of the film thickness to 4 nm, which was achieved for high-molecular mass s-PMMA ($\overline{M}_n = 880 \times 10^3$ g/mol), revealed another critical thickness below which the dielectric α -process, *i.e.* the cooperative glass transition dynamics, was found to disappear. In this work we present for the first time dielectric relaxation data on polymer trilayer (TL) films in which a dielectrically active polymer (isotactic PMMA or i-PMMA) is sandwiched between thin layers of a second, incompatible polymer (PS) with $T_g \sim 97$ °C which is approximately 40 °C higher than that of i-PMMA ($T_g \sim 56$ °C [10]). The purpose of the three-layer polymer film configuration is to reduce effects that are typically produced at a polymer-solid interface: specific interactions, *e.g.* hydrogen bonding of the PMMA chains with a substrate; and local chain orientations that are typical of polymer-solid interfaces. Instead, the central PMMA layer of the trilayer film has diffuse but well-defined polymer-polymer interdiffusion layers. For the specific combination PS–PMMA, an interfacial thickness of 4–5 nm has been determined using neutron reflectivity [24] and direct nonradiative energy transfer (DET) fluorescence decay experiments [25]. Taking advantage of the absence of strong dielectric loss processes in PS, the dielectric spectra of the trilayers represent exclusively the dynamics of the central PMMA film together with PMMA chains that contribute to the diffuse interfacial layers between the PMMA and PS films.

2 Experimental

Ultrathin single layer (SL) polymer films were prepared from i-PMMA ($\overline{M}_n = 118 \times 10^3$ g/mol, $\overline{M}_w/\overline{M}_n = 1.12$, Polymer Source Inc., Quebec) by spincoating on cleaned glass slides onto which a $\sim(40 \pm 10)$ nm thick layer of aluminium had been evaporated. By varying the concentration of the polymer solution between 0.2 and 4.0% and the spin speed between 2000 and 4000 rpm, films of uniform thickness with thicknesses between 6 nm and about 200 nm were obtained. Following the deposition and annealing of the PMMA films at 105 °C, Al was evaporated at a high deposition rate of ~ 10 nm/s onto the PMMA to form a patterned top electrode [10]. For the preparation of trilayer (TL) samples, the lower PS film (75 nm, $\overline{M}_n = 641 \times 10^3$ g/mol) was spincoated onto the metallised substrate, and the middle i-PMMA film and the upper PS-film were spincoated on mica sheets. After annealing the films under vacuum for 12 h at $T = 115$ °C (PS) or $T = 80$ °C (i-PMMA), the i-PMMA films and the

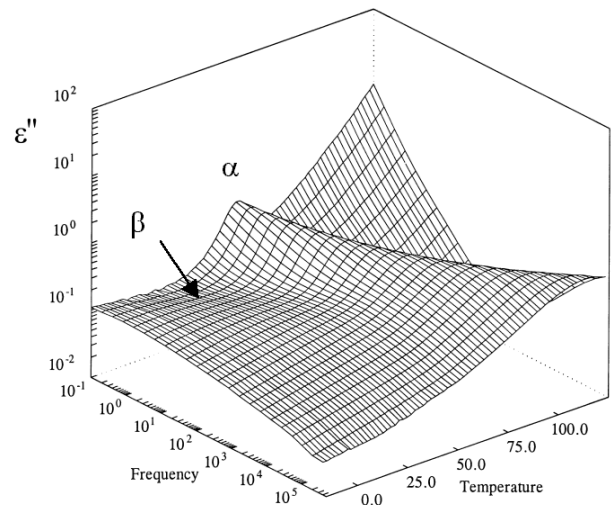


Fig. 2. Dielectric loss $\epsilon''(f, T)$ of a relatively thick single layer film of i-PMMA ($L = 58$ nm).

upper PS film were floated onto the lower PS film using a water transfer technique [5]. After assembling, the resulting trilayer films were kept in a dry container prior to the dielectric experiments, which were carried out upon slow cooling, always starting with an annealing step for approximately 1 h at $T = 120$ °C in dry gaseous nitrogen to remove residual moisture and relax mechanical stresses in the TL sample. DRS experiments in the frequency range from 10^{-1} to 10^6 Hz were performed with a custom-made dielectric spectrometer using a RLC-meter HP4284A, and a Schlumberger 1260 or a Stanford Research DSP lock-in 830 in combination with a high-impedance dielectric interface. The sample temperature was controlled by a Novocontrol Quatro Cryosystem and a Eurotherm 808P temperature controller.

3 Results and discussion

Figure 2 shows the 3D-representation of the dielectric loss $\epsilon''(f, T)$ for a relatively thick i-PMMA SL film ($L = 58$ nm), which clearly reveals the dielectric α -process related to the dynamic glass transition, and the β -process of i-PMMA, which is associated with local motions predominantly involving the side groups.

To analyse the dielectric spectra, various strategies were employed which are described in detail elsewhere [26,27]. In this paper we will restrict ourselves to the discussion of changes in the position (*e.g.* peak maximum temperatures T_{\max}) and the width of the relaxation process as a function of the sample thickness in both the SL and TL geometries.

First we focus on the shape of the loss peaks which can be visualised in masterplots obtained by horizontal shifting and normalisation to ϵ''_{\max} of the loss curves as shown in Figures 3 and 4. With decreasing film thickness, the α -peak broadens with both the low temperature and high temperature slopes becoming smaller. A broadening of the

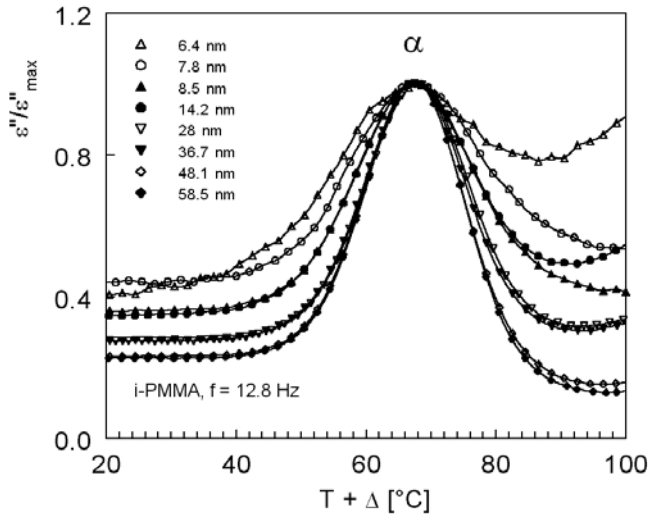


Fig. 3. Normalized dielectric loss $\epsilon''(T)/\epsilon''(T_{\max})$ of i-PMMA single layer films for $f = 12$ Hz additionally shifted to the peak position T_{\max} of the thickest film ($L = 58$ nm).

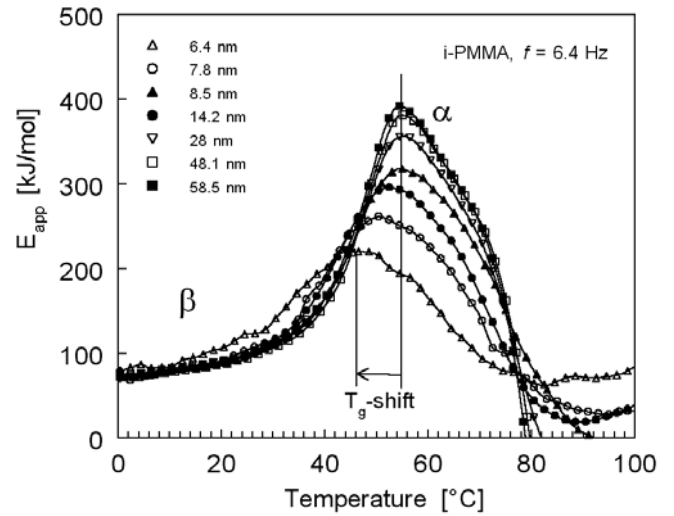


Fig. 5. Apparent activation energy $E_{\text{app}}(T)$ for i-PMMA in a single layer geometry for various thicknesses.

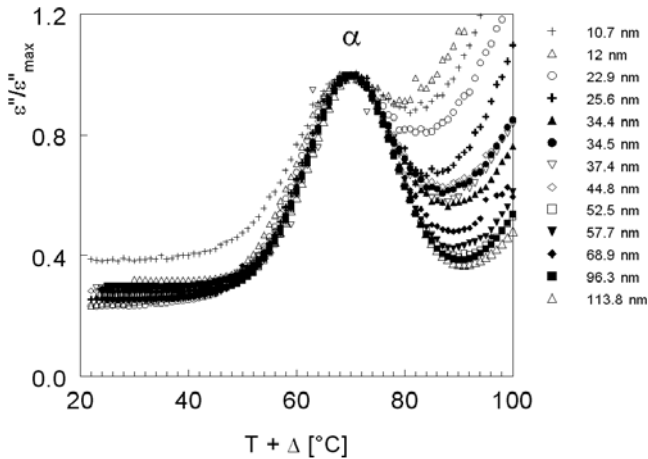


Fig. 4. Analogue representation of the dielectric loss $\epsilon''(T)/\epsilon''(T_{\max})$ of i-PMMA evaluated from the PS-PMMA-PS trilayer spectra ($f = 12$ Hz).

α -relaxation can generally be attributed to either changes in the intrinsic spectral shape of the α -process (*e.g.* due to changes in the intermolecular cooperativity [18]) or to a spatial distribution of regions having different, local non-broadened dynamics. A good criterion to distinguish between these two scenarios is the change in the low-frequency slope of the loss peak (in double-logarithmic representation) compared to the high-frequency slope. For a given polymer structure, the fast part of the glass transition dynamics, represented by the high-frequency slope, is determined by the short-range, intramolecular interactions [28], whereas the slow dynamics (related to the low-frequency slope) is sensitive to intermolecular interactions, *i.e.* to the degree of cooperativity, which is usually correlated to the fragility. Hence, changes in the fragility as recently found by Fukao for ultrathin films of PS [29] will most likely only have an effect on the low-frequency part of α -peak, while the high-frequency slope remains unaltered.

In contrast, a broadened α -peak originating from individually non-broadened contributions having a distribution in their mean relaxation time would necessarily result in a symmetric change of the peak shape. This effect is clearly seen for the α -process in i-PMMA SL films which strongly suggests that there is a spatially inhomogeneous cooperative mobility. Comparing Figures 3 and 4 further shows that this peak broadening is clearly more pronounced for PMMA single layers than for PMMA layers of comparable thickness sandwiched between PS layers. This observation implies that the glass transition dynamics of i-PMMA are more spatially homogeneous in the presence of diffuse PS-PMMA interfaces.

The second, even more important, effect of the thickness reduction is the shift in the glass transition temperature T_g . To deduce T_g values from the dielectric experiments we have applied the so-called activation energy fine-structure analysis [26] which yields the local, apparent activation energy $E_{\text{app}}(T)$ from the dielectric spectra $\epsilon'(f, T)$. It has been demonstrated earlier that this technique yields a “dielectric” T_g corresponding to the maximum position in $E_{\text{app}}(T)$ which is usually close to the calorimetric and dilatometric glass transition temperature within 1–2 °C [30]. The $E_{\text{app}}(T)$ curves for i-PMMA are given in Figure 5 (SL films) and Figure 6 (TL films). The $T_g(L)$ data are displayed in Figure 7 together with the loss peak maximum temperatures at 12 Hz and 13 kHz. Although the T_g values obtained from $E_{\text{app}}(T)$ are systematically lower than the loss peak temperatures $T(\epsilon''_{\max})$, $T_g(E_{\text{app}})$ and $T(\epsilon''_{\max})$ at 12 Hz show the same trend in the thickness dependence. However, in contrast to the T_g -reductions with decreasing film thickness L found for i-PMMA SL films, trilayer samples reveal the opposite trend of a slight increase in T_g upon decrease in L . This qualitative difference in behaviour must have its origin in the role of the surface regions of the PMMA films, which is fundamentally different in the two sample geometries: attractive, hard metal boundaries (Al electrodes) for

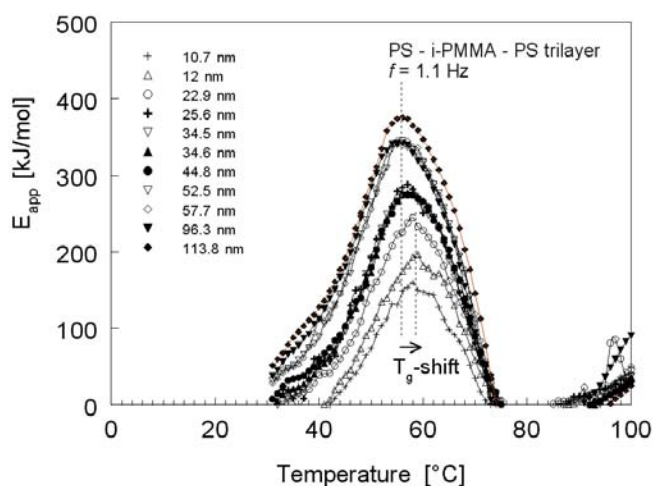


Fig. 6. Apparent activation energy $E_{app}(T)$ for i-PMMA in a trilayer geometry for various thicknesses.

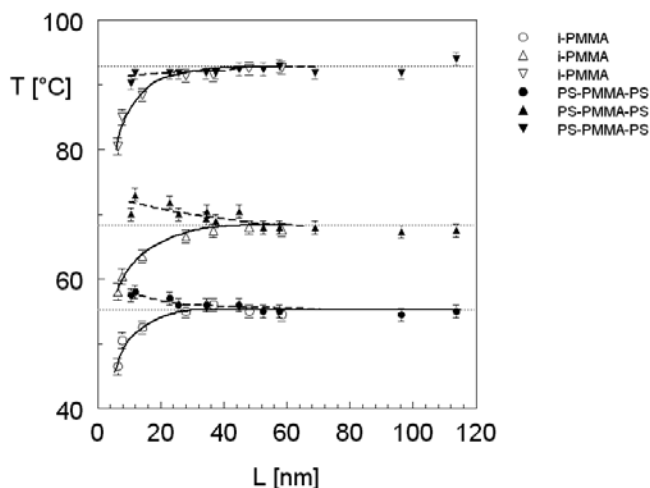


Fig. 7. Peak maximum temperatures $T(\epsilon''_{max})$ at $f = 13$ kHz (top) and 12 Hz (middle), and T_g obtained from the apparent activation energy $T_g(E_{app})$ at 6.4 Hz for SL films and 1.1 Hz for TL films (bottom) for i-PMMA as a function of the film thickness. The dotted lines correspond to the values measured for the thickest films and all other lines are intended to guide the eye.

the SL films *versus* diffuse polymer-polymer interfaces for the TL films. We suggest two possible mechanisms for the $T_g(L)$ trend in the trilayer samples: a) a contribution of the PS-PMMA interface region having a slower dynamics because $T_g(\text{PS}) \approx 97^\circ\text{C} > T_g(\text{i-PMMA}) = 56^\circ\text{C}$, and b) a reduced role of surface-induced chain orientations and conformational modifications due to the absence of a hard wall boundary for PMMA chains. Further studies to confirm these ideas are in progress.

References

1. J.L. Keddie, R.A.L. Jones, R.A. Cory, *Europhys. Lett.* **27**, 59 (1994)
2. K. Dalnoki-Veress, J.A. Forrest, C.A. Murray, C. Gigault, J.R. Dutcher, *Phys. Rev. E* **63**, 031801 (2001)
3. S. Kawana, R.A.L. Jones, *Phys. Rev. E* **63**, 021501 (2001)
4. J.A. Forrest, K. Dalnoki-Veress, J.R. Stevens, J.R. Dutcher, *Phys. Rev. Lett.* **77**, 2002 (1996)
5. J.A. Forrest, K. Dalnoki-Veress, J.R. Dutcher, *Phys. Rev. E* **56**, 5705 (1997)
6. J. Mattsson, J.A. Forrest, L. Borjesson, *Phys. Rev. E* **62**, 5187 (2000)
7. J.H. van Zanten, W.E. Wallace, W.-L. Wu, *Phys. Rev. E* **53**, R2053 (1996)
8. O.K.C. Tsui, T.P. Russell, C.J. Hawker, *Macromolecules* **34**, 5535 (2001)
9. K. Fukao, S. Uno, Y. Miyamoto, A. Hoshino, H. Miyaji, *Phys. Rev. E* **64**, 051807 (2001)
10. M. Wübbenhorst, C.A. Murray, J.A. Forrest, J.R. Dutcher, *Proc. of 11th International Symposium on Electrets*, 1–3 October Melbourne, Australia, 401 (2002)
11. L. Hartmann, W. Gorbatschow, J. Hauwede, F. Kremer, *Eur. Phys. J. E* **8**, 145 (2002)
12. A.M. Mayes, *Macromolecules* **27**, 3114 (1994)
13. K. Tanaka, A. Taura, S.-R. Ge, A. Takahara, T. Kajiyama, *Macromolecules* **29**, 3040 (1996)
14. J.A. Forrest, J. Mattson, *Phys. Rev. E* **61**, R53 (2000)
15. S. Herminghaus, *Eur. Phys. J. E* **5**, 531 (2001); S. Herminghaus, *Eur. Phys. J. E* **8**, 237 (2002)
16. P.G. de Gennes, *Eur. Phys. J. E* **2**, 201 (2000)
17. K.L. Ngai, A. Rizos, *Mater. Res. Soc. Proc.* **455**, 147 (1997)
18. K.L. Ngai, *Eur. Phys. J. E* **8**, 225 (2002)
19. D. Long, F. Lequeux, *Eur. Phys. J. E* **4**, 371 (2001)
20. G.B. McKenna, *J. Phys. IV France* **10**, Pr7–53 (2000)
21. Y. Grohens, L. Hamon, G. Reiter, A. Soldera, Y. Holl, *Eur. Phys. J. E* **8**, 217 (2002)
22. O.K.C. Tsui, H.F. Zhang, *Macromolecules* **34**, 9139 (2001)
23. P. Bernazzani, S.L. Simon, D.J. Plazek, K.L. Ngai, *Eur. Phys. J. E* **8**, 201 (2002)
24. M. Sferrazza, C. Xiao, R.A.L. Jones, D.G. Bucknall, J. Webster, J. Penfold, *Phys. Rev. Lett.* **78**, 3693 (1997)
25. Y. Rharbi, M.A. Winnik, *Macromolecules* **34**, 5238 (2001)
26. J. van Turnhout, M. Wübbenhorst, *J. Non-Cryst. Solids* **305**, 50 (2002)
27. M. Wübbenhorst, J. van Turnhout, *J. Non-Cryst. Solids* **305**, 40 (2002)
28. A. Schönhals, E. Schlosser, *J. Non-Cryst. Solids* **131**, 1161 (1991)
29. K. Fukao, Y. Miyamoto, *J. Phys. IV France* **10**, Pr7–243 (2000)
30. I.J.A. Mertens, M. Wübbenhorst, W.D. Oosterbaan, L.W. Jenneskens, J. van Turnhout, *Macromolecules* **32**, 3314 (1999)